

Supporting Information

New insights into the GABA_A receptor structure and orthosteric ligand binding: Receptor modeling guided by experimental data

Tommy Sander, Bente Frølund, Anne Techau Bruun, Ivaylo Ivanov, J. Andrew McCammon, and Thomas Balle*.

* Corresponding author. Email: tb@farma.ku.dk.

METHODS

Model building

The homology modeling process was conducted in three steps as outlined below: 1) generation of initial models, 2) sampling of the β 5-L5' loop and F-loop, and 3) building the refined model based on the two previous steps. The program Modeller 9v7¹ was used in all runs and was setup to perform a thorough (*slow*) refinement. When building the entire α ₁ β ₂ γ ₂ pentamer, i.e. steps 1 and 3, Modeller's *automodel* class was used. Symmetry restraints were imposed on the refinement process to ensure (nearly) identical pairs of β ₂ α ₁ interfaces, defined as: β ₂ residues D24-P34, V53-D56, D95-F105, A135-R141, E153-I164 and K196-R207, and α ₁ residues D9-D19, L22, D43-P51, T60-R66, V82-M89, K92, N110-L117, L127-T133 and T171-Y190. For loop sampling, the *loopmodel* class in Modeller was used.

- 1) Four hundred initial models were generated based on the alignment shown in main article Figure 2, so that only certain templates were used in certain regions, as indicated in the figure. Residue specific restraints were imposed as outlined in Table S.I.-1. Two models (no. 53 and 226, referred to as models 1a and 1b, respectively) were selected for further use. Using the amino acid rotameric library implemented in the molecular modeling program Maestro v. 9.0,² residue R66 in all α ₁ chains was put in a conformation so that its guanidinium head group was inside the putative binding pocket, in accordance with reports in the literature.³⁻⁵ A resulting steric repulsion with α ₁ F45 was relieved by putting this residue in another energetically favorable conformation, likewise from Maestro's rotameric library, with a χ ₁ torsion angle of $\sim 180^\circ$ (identical to what is seen for the similar Y23 residue in the GLIC structure aligning with this position in GABA_AR).
- 2) In the second step, three rounds of loop sampling of the initial models were performed, namely, a) of the F-loop of the α ₁ subunit, b) of the β 5-L5' loop segment in the α ₁ subunit, and c) of the β 5-L5' loop segment in the γ ₂ subunit. In each run, 500 loop models were generated.

- a. Sampling of the F-loop (residues α_1 E169-L187) was performed on the β_2 - α_1 dimer (chains A-B) of the initial model 1a, imposing residue specific distance restraints as specified in Table S.I.-1. The α_1 subunit of the best model chosen for further use (no. 417) is referred to as model 2a.
 - b. Sampling of the α_1 β_5 -L5' loop (residues H109-K116) was performed on the β_2 - α_1 - β_2 trimer (chains A-B-C) of the initial model 1b. The α_1 subunit of the resulting best model (no. 381) is referred to as model 2b.
 - c. The loop conformation of model 2b was inserted in the α_1 and β_2 subunits of the initial model 1b, and in β_2 chains the loop residues were manually mutated to those found in the β_2 sequence. The α_1 - γ_2 - β_2 trimer (chains D-E-A) from this structure was now used in a similar round of sampling of the γ_2 β_5 -L5' loop (residues A119-M130). Residue specific restraints were imposed on the γ_2 loop sampling as outlined in Table S.I.-1. The γ_2 subunit of the model selected as the best from this sampling (no. 358) is referred to as model 2c.
- 3) In the final homology modeling step, 400 models of the GABA_A receptor EC domain were built using the selected models from steps 1 and 2 as templates. The primary templates were model 1a for β_2 , and model 1b for α_1 and γ_2 subunits because the best geometry and ProSA z-scores were obtained for the respective model-subunit combinations. For a few short regions the roles were switched so that model 1a was used for α_1 , and model 1b for β_2 , because here the backbone conformation was flipped for some residues relative to the original structural templates. Model 2a acted as template for the F-loop in all five subunits, model 2b as template for the β_5 -L5' loop in α_1 and β_2 chains, and model 2c as template for the β_5 -L5' loop in γ_2 . Specific details of which templates were used in which regions can be found in Fig. S.I.-1. Of the generated models, no. 193 was selected as the overall best (see Table S.I.-2) and is referred to as the refined model (see selection criteria in the main article). Backbone conformations resulting in Ramachandran plot violations (three residues in loop regions, none near the orthosteric or BZD binding sites) were manually adjusted to the proper configuration using the “rotate peptide plane” tool in Maestro. The model was treated according to the Protein Preparation procedure⁶ using exhaustive sampling of H-bond networks and otherwise standard settings. This procedure adds hydrogen atoms, connects disulfides, probes the optimal flip orientation and tautomeric state of glutamine, asparagine and histidine residues, optimizes H-bond networks, and performs a geometry optimization to a maximum RMSD of 0.3Å. The N- and C-termini were modeled in their protonated ammonium and deprotonated carboxylate states, respectively, and all basic and acidic residues were in their default protonated states (neutral His, protonated Arg and Lys, and deprotonated Asp and Glu).

Molecular Dynamics (MD)

An MD simulation of the refined GABA_AR model after the above mentioned geometry optimization was set up and carried out in explicit solvent consisting of TIP3P type⁷ water molecules. Initially, the program GRID^{8,9} was used to place water molecules in favorable areas throughout the structure, using the water probe (OH2) and a grid spacing of 0.5 Å (*NPLA*=2) to calculate interaction energies between protein and water, and minima below -5 kcal/mol were occupied. A total of 1855 water molecules were added and subsequently geometry optimized around the model with all protein atoms kept frozen in space. This complex was centered in a cubic box with side lengths of 114.5 Å, corresponding to a 15 Å buffer distance between the protein and each side of the box, which was filled with an additional 40,214 waters as well as with 113 Na⁺ and 112 Cl⁻ ions to neutralize the system and afford a ~0.15M solution resembling physiological conditions. The system was setup with periodic boundary conditions and comprised in total 42,258 molecules, or 143,490 atoms.

The 12-step MD protocol comprising two rounds of energy minimization, nine equilibration steps and a production run was as follows:

- 1) Minimization with 50 kcal/mol/Å² position restraints on protein atoms. 10 steps of steepest descent followed by conjugate gradient until convergence at 50 kcal/mol/Å.
- 2) Minimization like above but without position restraints. Convergence at 5 kcal/mol/Å.
- 3) 12 ps at 10 K in the NVT ensemble, time steps of 1:1:3 fs (bonded:near:far interactions), protein heavy atoms restrained with 50 kcal/mol/Å².
- 4) 24 ps at 10 K, protein heavy atoms restraints kept.
- 5) 60 ps at 300 K, protein heavy atoms restraints kept.
- 6) 120 ps, protein heavy atoms restraints lowered to 5 kcal/mol/Å².
- 7) 120 ps, protein Cα's restrained with 5 kcal/mol/Å², side chain heavy atoms with 1 kcal/mol/Å².
- 8) 120 ps, Cα restraints kept, side chains released.
- 9) 120 ps, Cα restraints lowered to 3 kcal/mol/Å².
- 10) 120 ps, Cα restraints lowered to 1 kcal/mol/Å².
- 11) 9.6 ns, Cα restraints lowered to 0.25 kcal/mol/Å².
- 12) 48 ns production run.

As is the default in the used MD program (Desmond), pressure and temperature during the equilibration steps 3-11 were coupled with the Berendsen methods¹⁰ (only temperature in step 3 where the default constant-NVT ensemble was used). During the production run, the Nosé-

Hoover thermostat¹¹ and Martyna-Tobias-Klein barostat¹² were used. Unless specifically stated above, default Desmond settings were used: OPLS 2005 force field, constant-NPT ensemble at 1 atm pressure and 300 K temperature, 2:2:6 fs integration steps (bonded:near:far interactions, where “far” is > 9Å), constrained covalent bonds between heavy atoms and hydrogens using the SHAKE algorithm,¹³ and smooth particle mesh Ewald electrostatics¹⁴ beyond the short range Coulombic interactions cutoff at 9Å. The use of shorter integration time steps in step 3 is standard procedure in Desmond in the initial heating step.

Similar MD simulations were performed for the *Ac*-AChBP apo structure (PDB: 2byn) and the EC domain of the ELIC structure (PDB: 2v10, chains A-E). Non-protein molecules and moieties were deleted from the *Ac*-AChBP structure, as were the N-terminal FLAG epitopes so that each chain sequence started with 1-HSQ. For the ELIC structure, the transmembrane part starting at residues 200-PSY was deleted from each chain in the original PDB structure. The two pentamers were treated like the GABA_AR model as described above (protein preparation, GRID solvation etc.). The MD protocol outlined above was followed with the exceptions that, 1) the production runs were terminated after 30.0 ns for *Ac*-AChBP and 35.6 ns for ELIC, and 2) for *Ac*-AChBP, equilibration steps 9-11 were only run for 60 ps, 60 ps, and 120 ps, respectively.

DISCUSSION

Alignment considerations and alterations

A proper sequence alignment is perhaps the single most critical step in homology modeling.¹⁵ In some regions of the GABA_AR sequences there is little consensus in the literature as to how they should align with the other Cys-loop receptors.¹⁶⁻²³ With sequence identities between the GABA_AR and templates falling in the low range of 13-18% (calculated with BioEdit²⁴ using the alignment in Figure 2 of the main text), special attention was required in this phase. We settled on an iterative protocol where a thoroughly verified structural alignment of the templates was expanded by adding all human nAChR sequences because of their close relation to the mouse and *Torpedo* nAChR structures, and finally adding the human GABA_AR sequences. Motifs that are conserved among the different Cys-loop receptor subfamilies were thus better identified. However, we still found that manual alterations were needed because such motifs were not always properly caught by the automated procedure (in our case the ClustalX program), and because certain regions with poor sequence similarity were inappropriately aligned.

As stated in the Methods section of the main manuscript, manual adjustments were made in four regions, namely, 1) in and after the N-terminal α -helix, 2) in the L5- β 5' segment, 3) in loop F, and 4) in loop C. The rationale behind this is described in the following (a detailed comparison of the sequence alignments before and after the alterations is given in Fig. S.I.-2).

At the N-terminal part highly conserved motifs corresponding to the GABA_AR α_1 sequence ¹⁷ILDRLLDGYDNRLLRP were misaligned by ClustalX. This was due to the presence of sequences in the alignment with insertions in this region (*Bt*-AChBP, *Torpedo* δ subunit, and human nAChR β_2 , β_4 and δ subunits). Manually altering the alignment not only reestablished these motifs at the sequence level, but also facilitated that the highly conserved Tyr residue corresponding to α_1 Y25 was positioned in the model so that it interacts with the likewise highly conserved α_1 D71 at the end of the β_2 strand, which would otherwise pack in hydrophobic surroundings. The same interaction is observed in the mouse nAChR α_1 structure, and hence we are confident that the altered alignment is correct.

In the L5- β 5' segment, between the absolutely conserved residues P96 and G124 (GABA_AR α_1 numbering), two-four extra residues are found in all GABA_AR subunits compared to the other Cys-loop sequences. We kept the insertions before the β 5' strand in order to align α_1 R119 (conserved among all GABA_AR subunits) with *Ls*-AChBP R104, hence facilitating the salt bridge formation described above for e.g. the α_1 R119... β_2 D163 ion pair. The actual position of the insertion was chosen arbitrarily and probably had minimal impact on the final model due to the subsequent loop sampling performed on this segment.

The long loop F between α_1 W170 and α_1 Y190 is particularly challenging as it has virtually no conserved regions among the Cys-loop family members, and in addition the structural templates have markedly different conformations of this loop. Therefore, we used the cysteine accessibility data reported by Newell & Czajkowski²⁵ to guide the alignment so that the initial models were in reasonable accordance with the observations of that study. Like for the β 5- β 5' segment this has probably only had minor impacts on the final structure because of the subsequent loop sampling. As our primary focus was on the orthosteric binding site, no attempts were made to optimize loop F in a similar way specifically for the β_2 and γ_2 subunits. We therefore chose to let their sequences follow that of the α_1 as closely as possible while making sure that hydrophobic packing of hydrophilic/charged residues did not occur.

Loop C in GABA_AR subunits is two to three residues shorter than in the relevant templates (i.e. the AChBPs, mouse α_1 , and *Torpedo* α subunit) and hence presents an important challenge in the alignment process. Main fix points were β_2 F200 and Y205 which align with highly conserved aromatic residues. The *Ac*-AChBP segment ¹⁸⁸YSCCPEPY was aligned with β_2 ²⁰⁰FS--TGSY, rather than ²⁰⁰FSTGS--Y as in the initial ClustalX alignment. This afforded a C-loop with good backbone geometry (i.e. in favored/allowed areas in the

Ramachandran plot) and with β_2 T202 facing the binding site. This is in apparent accordance with experimental data demonstrating that in this position a residue with a hydroxyl group (Thr or Ser) is pivotal for activating the receptor with GABA or muscimol.^{26,27}

It should be noted that the vast amount of experimental data that have been published for the GABA_AR receptor is not always easy to interpret, may sometimes appear contradictory, and hence should be interpreted with caution. For instance, in one of the studies referred to above for loop C,²⁷ residues β_2 F200-T202 were found to be solvent inaccessible, and the authors further concluded that they do not line the binding site. This is not compatible with our model. However, regardless of which alignment (if any) is correct for the above mentioned loop C stretch, the β_2 F200 residue does with high probability align with a tyrosine conserved among AChBP and nAChR sequences (and also ELIC) that clearly lines the binding site and directly engages in ligand binding. Similar uncertainties likely apply to the other parts of the model where such data were taken into consideration, e.g. in α_1 loop F. However for this region, in contrast to loop C, we have neither a reliable structural basis from the templates nor any contradictory results to question the biochemical data of Newell & Czajkowski,²⁵ so here priority was given to optimize adherence to their results.

In general we believe that the above summarized manual adjustments to the automatically generated sequence alignment are reasonable and have resulted in a more realistic GABA_AR model.

Table S.I.-1. Atom specific distance restraints imposed in model building.

Atom 1 ^a	Atom 2	Form ^b	Distance (std.dev.)
<i>Pentamer generation restraints (steps 1 and 3)</i>			
α_1 D54 C γ ^c	α_1 R220 C ζ	G	4.2 Å (0.1 Å)
α_1 R119 C ζ ^d	β_2 D163 C γ	G	4.2 Å (0.1 Å)
β_2 E153 C δ	β_2 K196 N ζ	G	3.3 Å (0.1 Å)
α_1 R73 C ζ ^d	α_1 L118 C β	L.b.	18 Å (1 Å)
β_2 R86 C ζ	β_2 L118 C β	L.b.	9 Å (0.5 Å)
β_2 Y97 C ζ ^d	β_2 L99 C β	U.b.	4.2 Å (0.1 Å)
β_2 Y97 C $\delta 2$ ^d	β_2 E155 C α	U.b.	5.0 Å (0.1 Å)
β_2 D95 O $\delta 1$ ^d	β_2 S156 O γ	U.b.	2.8 Å (0.1 Å)
β_2 D95 O $\delta 2$ ^d	β_2 Y157 N	U.b.	3.0 Å (0.1 Å)
β_2 D95 O $\delta 2$ ^d	β_2 G158 N	U.b.	3.0 Å (0.1 Å)
<i>F-loop sampling restraints</i>			
α_1 W170 C $\zeta 3$ ^{d,e}	α_1 I44 C β	U.b.	5.0 (0.1 Å)
α_1 A175 C β	α_1 I44 C β	U.b.	5.5 Å (0.3 Å)
α_1 S177 C β	β_2 Y157 C α	L.b.	21 Å (0.3 Å)
α_1 V178 C β	β_2 Y157 C α	U.b.	17.5 Å (0.3 Å)
α_1 V178 C β	α_1 V197 C β	L.b.	11 Å (0.3 Å)
α_1 V179 C β	α_1 I44 C β	U.b.	9.0 Å (0.3 Å)
α_1 V179 C β	α_1 V46 C β	L.b.	5.5 Å (0.3 Å)
α_1 V180 C β	β_2 Y157 C α	U.b.	20 Å (0.3 Å)
α_1 V180 C β	β_2 R207 C α	U.b.	20 Å (0.3 Å)
α_1 V180 C β	α_1 V46 C β	L.b.	9.0 Å (0.3 Å)
α_1 V180 C β	α_1 L192 C β	L.b.	8.0 Å (0.3 Å)
α_1 A181 C β	β_2 L99 C β	L.b.	17 Å (0.3 Å)
α_1 D183 C γ	β_2 R207 C α	U.b.	15.5 Å (0.3 Å)
<i>$\beta 5$-$\beta 5'$ loop sampling (γ_2 subunit)</i>			
γ_2 W123 C $\zeta 3$	γ_2 L143 C $\delta 1$	U.b.	5.0 Å (0.1 Å)
γ_2 I124 C α	γ_2 R144 C β	U.b.	7.0 Å (0.1 Å)
γ_2 M130 C β	γ_2 T142 C β	U.b.	4.5 Å (0.1 Å)

^a Atom specification format: subunit - residue - *PDB atom name*.

^b The Modeller distance restraint type enforced. G, Gaussian; U.b., Upper bound; L.b., Lower bound.

^c Also set for the corresponding residues/atoms in β_2 subunits.

^d Also set for the corresponding residues/atoms in the other subunits.

^e Also imposed as restraint in the final model building step

Table S.I.-2. Modeller *molpdf* and DOPE scores, ProSA z-scores, and OPLS 2001 energies of all homology models top ranked in either Modeller score or within top 50 of both. Highlighted rows indicate models selected for further use from each run.

Model no.	Modeller scores		ProSA z-score (by chain and weighted average)					Avg ^b	OPLS 2001 energy (kcal/mol) ^c
	<i>molpdf</i> ^a	DOPE	A / β_2	B / α_1	C / β_2	D / α_1	E / γ_2		
<i>Initial model generation</i>									
53 (1a)	29715	-112206	-3.80	-4.92	-3.85	-4.43	-4.43	-4.29	478
79	29909	-111935	-3.72	-4.92	-3.72	-5.05	-4.52	-4.39	559
99	29809	-112522	-3.67	-5.15	-3.84	-5.06	-4.34	-4.41	483
163	29850	-112693	-3.41	-4.88	-3.90	-4.91	-4.46	-4.31	478
205	29490	-110644	-3.82	-4.39	-3.92	-4.31	-4.74	-4.24	543
226 (1b)	29697	-112143	-3.66	-5.17	-3.76	-5.05	-4.68	-4.47	470
262	30245	-113466	-3.80	-5.17	-3.82	-5.06	-4.60	-4.49	494
367	29621	-111940	-3.87	-5.04	-3.77	-4.97	-4.48	-4.43	501
398	29899	-111993	-3.77	-4.79	-3.79	-4.54	-4.62	-4.30	502
<i>F-loop sampling (α_1 subunit)^d</i>									
24	68.7	-1799	-	-5.32	-	-	-	-	203
33	69.3	-1866	-	-5.38	-	-	-	-	188
38	77.1	-1878	-	-5.38	-	-	-	-	188
70	70.3	-1866	-	-5.29	-	-	-	-	190
74	60.4	-1874	-	-5.20	-	-	-	-	189
98	78.5	-1803	-	-5.14	-	-	-	-	189
195	48.5	-1849	-	-5.33	-	-	-	-	192
207	59.2	-1902	-	-5.17	-	-	-	-	186
219	80.7	-1811	-	-5.18	-	-	-	-	192
225	61.2	-1834	-	-5.36	-	-	-	-	196
250	82.9	-1825	-	-5.13	-	-	-	-	193
271	50.8	-1929	-	-5.12	-	-	-	-	191
275	70.7	-1908	-	-5.01	-	-	-	-	193
276	58.8	-1900	-	-5.22	-	-	-	-	187
313	77.7	-1816	-	-5.24	-	-	-	-	189
345	59.2	-1781	-	-4.98	-	-	-	-	192
351	64.5	-1882	-	-5.28	-	-	-	-	191
407	12.6	-1793	-	-5.17	-	-	-	-	187
417 (2a)	75.6	-1966	-	-5.41	-	-	-	-	185
436	68.5	-1916	-	-5.32	-	-	-	-	188

Model no.	Modeller scores		ProSA z-score (by chain and weighted average)					Avg ^b	OPLS 2001 energy (kcal/mol) ^c
	<i>molpdf</i> ^a	DOPE	A / β_2	B / α_1	C / β_2	D / α_1	E / γ_2		
469	76.1	-1810	-	-5.34	-	-	-	-	193
471	320.0	-1978	-	-5.27	-	-	-	-	239
<i>β_5-L5' loop sampling (α_1 subunit)^e</i>									
9	22.4	-1121	-	-5.11	-	-	-	-	295
10	12.4	-1250	-	-5.07	-	-	-	-	297
64	25.3	-1155	-	-4.90	-	-	-	-	293
96	21.2	-1152	-	-5.08	-	-	-	-	297
97	1095.0 ^f	-1305	-	-5.01	-	-	-	-	302
108	8.4	-1190	-	-5.09	-	-	-	-	299
115	16.2	-1185	-	-5.08	-	-	-	-	299
117	20.7	-1237	-	-5.13	-	-	-	-	293
122	19.8	-1206	-	-5.08	-	-	-	-	297
183	23.6	-1166	-	-4.87	-	-	-	-	297
317	23.7	-1180	-	-5.10	-	-	-	-	294
318	23.2	-1195	-	-5.13	-	-	-	-	294
355	13.6	-1249	-	-5.05	-	-	-	-	299
364	22.5	-1187	-	-5.03	-	-	-	-	296
381 (2b)	26.9	-1202	-	-5.13	-	-	-	-	291
414	17.2	-1184	-	-5.10	-	-	-	-	293
465	22.0	-1190	-	-5.13	-	-	-	-	298
<i>β_5-L5' loop sampling (γ_2 subunit)^g</i>									
6	150.9	-2161	-	-	-	-	-4.82	-	305
49	23.7	-1984	-	-	-	-	-4.61	-	289
146	47.1	-2122	-	-	-	-	-4.81	-	301
165	27.5	-2116	-	-	-	-	-4.86	-	296
194	35.1	-2073	-	-	-	-	-4.72	-	284
321	33.1	-2068	-	-	-	-	-4.82	-	300
358 (2c)	32.6	-2143	-	-	-	-	-4.79	-	282
447	41.4	-2105	-	-	-	-	-4.90	-	290
499	44.9	-2089	-	-	-	-	-4.87	-	288
<i>Refined model generation</i>									
99	5611	-112296	-3.75	-5.32	-4.11	-5.75	-4.47	-4.68	491
100	5709	-112046	-4.01	-5.29	-4.08	-5.73	-4.58	-4.74	467

Model no.	Modeller scores		ProSA z-score (by chain and weighted average)					Avg ^b	OPLS 2001 energy (kcal/mol) ^c
	<i>molpdf</i> ^a	DOPE	A / β_2	B / α_1	C / β_2	D / α_1	E / γ_2		
112	5762	-112740	-4.25	-5.32	-4.09	-5.65	-4.78	-4.82	420
193	5651	-112350	-4.37	-5.30	-4.07	-5.83	-4.51	-4.82	413 ^h
354	5721	-112340	-3.95	-5.13	-4.03	-5.59	-4.44	-4.63	430
358	5542	-111242	-4.00	-4.93	-4.13	-5.47	-4.52	-4.61	488
359	5729	-112032	-3.82	-5.22	-4.05	-5.72	-4.50	-4.67	436
386	5637	-112102	-3.71	-5.29	-4.09	-5.78	-4.64	-4.71	455
396	5667	-112213	-4.18	-4.96	-4.28	-5.58	-4.45	-4.69	429

^a Note that the *molpdf* scores are incomparable between runs.

^b Average z-score per chain weighted after number of residues in each chain (α_1 , 213; β_2 and γ_2 , 211).

^c After being subjected to the Protein Preparation geometry optimization.⁶

^d The OPLS 2001 energy of the input dimer was 211 kcal/mol.

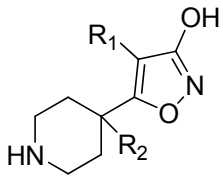
^e The OPLS 2001 energy of the input trimer was 307 kcal/mol.

^f The high *molpdf* for model 97 is due to the α_1 H109 imidazole ring having a severely distorted configuration with crossing covalent bonds. This was fixed prior to running pprep.

^g The OPLS 2001 energy of the input trimer was 291 kcal/mol.

^h OPLS 2001 energy before manually adjusting the three peptide bonds causing Ramachandran plot violations (see text). After adjustments the energy was 401 kcal/mol as reported in the main article. (ProSA z-scores were identical before and after adjustments)

Table S.I.-3. Structure, binding affinity and docking score (Glide Gscore²⁸) for the highest ranked docking pose of all 52 4-PIOL and 4-PHP derived ligands docked to the model binding site.

Compound ^a	R ₁	R ₂	K _i (μM)	Ref ^b	Gscore
					
1 (4-PIOL)	H	H	9.1	²⁹	-7.2
	H	methyl	37	²⁹	-7.0
	methyl	H	10	²⁹	-7.2
	ethyl	H	6.3	²⁹	-7.1
	propyl	H	6.6	²⁹	-6.8
	butyl	H	7.7	²⁹	-7.5
	hexyl	H	4.5	²⁹	-6.5
	octyl	H	1.8	²⁹	-5.2
	cyclohexyl	H	4.9	²⁹	-7.1
2	phenyl	H	0.22	³⁰	-7.4
3	benzyl	H	3.8	²⁹	-7.2
	2-phenylethyl	H	5.0	²⁹	-6.9
	3-phenylpropyl	H	1.1	²⁹	-7.5
	diphenylmethyl	H	0.96	²⁹	-6.9
	2,2-diphenylethyl	H	0.36	²⁹	-6.8
4	3,3-diphenylpropyl	H	0.068	²⁹	-7.8
	4,4-diphenylbutyl	H	0.70	²⁹	-8.4
5	3-biphenyl	H	0.010	³¹	-8.3
	4-biphenylmethyl	H	0.4	²⁹	-7.9
	1-naphthyl	H	0.82	³⁰	-7.3
	2-naphthyl	H	0.036	³⁰	-7.0
	1-naphthylmethyl	H	0.10	²⁹	-7.6
	1-naphthylethyl	H	1.7	²⁹	-7.6
6	2-naphthylmethyl	H	0.049	²⁹	-7.9
7	1-phenyl-2-naphthylmethyl	H	0.021	³⁰	-8.5
	1-fluoro-2-naphthylmethyl	H	0.019	³⁰	-7.9
	1-chloro-2-naphthylmethyl	H	0.016	³⁰	-7.8
	1-cyano-2-naphthylmethyl	H	0.028	³⁰	-8.0
	1-methylthio-2-naphthylmethyl	H	0.028	³⁰	-8.0
	1-phenylthio-2-naphthylmethyl	H	0.250	³⁰	-8.0
8	1-bromo-2-naphthylmethyl	H	0.011	³⁰	-7.5
9	5-bromo-2-naphthylmethyl	H	0.080	³⁰	-7.8

Compound ^a	R ₁	R ₂	K _i (μM)	Ref ^b	Gscore
10	7-bromo-2-naphthylmethyl	H	0.109	30	-7.8
11	8-bromo-2-naphthylmethyl	H	0.045	30	-7.7
	2-naphthylethyl	H	0.49	29	-7.9
	9-anthracylmethyl	H	5.9	29	-7.4

12 (4-PHP)	H	H	10	32	-7.4
	phenyl	H	0.022	32	-7.1
13	3-biphenyl	H	0.0028	32	-7.8
14	2-naphthylmethyl	H	0.033	32	-7.7
15	1-bromo-2-naphthylmethyl	H	0.0095	32	-7.3
	H	methyl	5.0	32	-7.5
	H	phenyl	0.27	32	-7.1
	H	2-tolyl	0.67	32	-7.2
	H	3-tolyl	0.24	32	-7.6
	H	4-tolyl	0.32	32	-7.1
	H	benzyl	0.36	32	-7.8
16	H	3-biphenyl	0.030	32	-8.5
17	H	4-biphenyl	0.42	32	-7.0
18	H	2-naphthylmethyl	0.0030	32	-8.9
	2-naphthylmethyl	phenyl	1.5	32	-7.8
19	phenyl	2-naphthylmethyl	0.022	32	-9.5

^a Compound number for those mentioned in the main article.

^b Literature reference for the given K_i value.

Fig. S.I.-1. Alignments of the initial models 1a-b and 2a-c to each chain sequence in the refined model, highlighting (in blue) which templates were used in which regions in step 3 of the homology modeling protocol. Model 1a and 1b sequences correspond to the relevant chain of the refined model. Models 2a and 2b are only α_1 sequences; model 2c is only γ_2 .

<i>model-1a</i>	9	DNTTVFTRILDRLLDGYDNRLRPLGERVTEVKTDIFVTSFGPVSDDHMEYTDVFFRQSWKDERLKFKGP	79
<i>model-1b</i>	9	DNTTVFTRILDRLLDGYDNRLRPLGERVTEVKTDIFVTSFGPVSDDHMEYTDVFFRQSWKDERLKFKGP	79
<i>model-2a</i>	9	DNTTVFTRILDRLLDGYDNRLRPLGERVTEVKTDIFVTSFGPVSDDHMEYTDVFFRQSWKDERLKFKGP	79
<i>model-2b</i>	9	DNTTVFTRILDRLLDGYDNRLRPLGERVTEVKTDIFVTSFGPVSDDHMEYTDVFFRQSWKDERLKFKGP	79
<i>refined-α_1</i>	9	DNTTVFTRILDRLLDGYDNRLRPLGERVTEVKTDIFVTSFGPVSDDHMEYTDVFFRQSWKDERLKFKGP	79
<i>model-1a</i>	80	MTVLRNLNLMASKIWTPTDFFHNGKKSVAHNMTMPNKLRLRITDGTLLYTMRLTVRAECPMHLEDFPMDAH	150
<i>model-1b</i>	80	MTVLRNLNLMASKIWTPTDFFHNGKKSVAHNMTMPNKLRLRITDGTLLYTMRLTVRAECPMHLEDFPMDAH	150
<i>model-2a</i>	80	MTVLRNLNLMASKIWTPTDFFHNGKKSVAHNMTMPNKLRLRITDGTLLYTMRLTVRAECPMHLEDFPMDAH	150
<i>model-2b</i>	80	MTVLRNLNLMASKIWTPTDFFHNGKKSVAHNMTMPNKLRLRITDGTLLYTMRLTVRAECPMHLEDFPMDAH	150
<i>refined-α_1</i>	80	MTVLRNLNLMASKIWTPTDFFHNGKKSVAHNMTMPNKLRLRITDGTLLYTMRLTVRAECPMHLEDFPMDAH	150
<i>model-1a</i>	151	ACPLKFGSYAYTRAEEVVEWTRPARSVVVAEDGSRLNQYDLLGQTVDSGIVQSSTGEYVVMTHHFLKRR	221
<i>model-1b</i>	151	ACPLKFGSYAYTRAEEVVEWTRPARSVVVAEDGSRLNQYDLLGQTVDSGIVQSSTGEYVVMTHHFLKRR	221
<i>model-2a</i>	151	ACPLKFGSYAYTRAEEVVEWTRPARSVVVAEDGSRLNQYDLLGQTVDSGIVQSSTGEYVVMTHHFLKRR	221
<i>model-2b</i>	151	ACPLKFGSYAYTRAEEVVEWTRPARSVVVAEDGSRLNQYDLLGQTVDSGIVQSSTGEYVVMTHHFLKRR	221
<i>refined-α_1</i>	151	ACPLKFGSYAYTRAEEVVEWTRPARSVVVAEDGSRLNQYDLLGQTVDSGIVQSSTGEYVVMTHHFLKRR	221
<i>model-1a</i>	7	SNMSLVKETVDRLKGYDIRLRPDFGGPPVAVGMNIDIASIDMVSEVNMDYTLTMYFQQAWRDKRLSYNVI	77
<i>model-1b</i>	7	SNMSLVKETVDRLKGYDIRLRPDFGGPPVAVGMNIDIASIDMVSEVNMDYTLTMYFQQAWRDKRLSYNVI	77
<i>model-2a</i>	9	DNTTVFTRILDRLLDGYDNRLRPLGERVTEVKTDIFVTSFGPVSDDHMEYTDVFFRQSWKDERLKFKGP	79
<i>model-2b</i>	9	DNTTVFTRILDRLLDGYDNRLRPLGERVTEVKTDIFVTSFGPVSDDHMEYTDVFFRQSWKDERLKFKGP	79
<i>refined-β_2</i>	7	SNMSLVKETVDRLKGYDIRLRPDFGGPPVAVGMNIDIASIDMVSEVNMDYTLTMYFQQAWRDKRLSYNVI	77
<i>model-1a</i>	78	PLNLTLDNRVADQLWVPDITYFLNDKKS FVHGVTVKNRMIRLHPDGTLYGLRITTTAACMMDLRRYPLDEQ	148
<i>model-1b</i>	78	PLNLTLDNRVADQLWVPDITYFLNDKKS FVHGVTVKNRMIRLHPDGTLYGLRITTTAACMMDLRRYPLDEQ	148
<i>model-2a</i>	80	MTVLRNLNLMASKIWTPTDFFHNGKKSVAHNMTMPNKLRLRITDGTLLYTMRLTVRAECPMHLEDFPMDAH	150
<i>model-2b</i>	80	MTVLRNLNLMASKIWTPTDFFHNGKKSVAHNMTMPNKLRLRITDGTLLYTMRLTVRAECPMHLEDFPMDAH	150
<i>refined-β_2</i>	78	PLNLTLDNRVADQLWVPDITYFLNDKKS FVHGVTVKNRMIRLHPDGTLYGLRITTTAACMMDLRRYPLDEQ	148
<i>model-1a</i>	149	NCTLEIESYGYTTDDIEFYWRGDDNAVTVGVTKI--ELPQFSIVDYKLITKKVVFSTGSPRLLSFLKLRN	217
<i>model-1b</i>	149	NCTLEIESYGYTTDDIEFYWRGDDNAVTVGVTKI--ELPQFSIVDYKLITKKVVFSTGSPRLLSFLKLRN	217
<i>model-2a</i>	151	ACPLKFGSYAYTRAEEVVEWTRPARSVVVAEDGSRLNQYDLLGQTVDSGIVQSSTGEYVVMTHHFLKRR	221
<i>model-2b</i>	151	ACPLKFGSYAYTRAEEVVEWTRPARSVVVAEDGSRLNQYDLLGQTVDSGIVQSSTGEYVVMTHHFLKRR	221
<i>refined-β_2</i>	149	NCTLEIESYGYTTDDIEFYWRGDDNAVTVGVTKI--ELPQFSIVDYKLITKKVVFSTGSPRLLSFLKLRN	217
<i>model-1a</i>	22	VPEGDVTVILNLLLEGYDNKLRPDIGVKPTLIHTDMYVNSIGPVNAINMEYTDIFFAQTWYDRRLKFNST	92
<i>model-1b</i>	22	VPEGDVTVILNLLLEGYDNKLRPDIGVKPTLIHTDMYVNSIGPVNAINMEYTDIFFAQTWYDRRLKFNST	92
<i>model-2a</i>	9	DNTTVFTRILDRLLDGYDNRLRPLGERVTEVKTDIFVTSFGPVSDDHMEYTDVFFRQSWKDERLKFKGP	79
<i>model-2c</i>	22	VPEGDVTVILNLLLEGYDNKLRPDIGVKPTLIHTDMYVNSIGPVNAINMEYTDIFFAQTWYDRRLKFNST	92
<i>refined-γ_2</i>	22	VPEGDVTVILNLLLEGYDNKLRPDIGVKPTLIHTDMYVNSIGPVNAINMEYTDIFFAQTWYDRRLKFNST	92
<i>model-1a</i>	93	IKVLRNLNSNMVGKIWIPTDFFRNSKKADAHWITTPNRMLRIWNDGRVLYTLRLTIDAECQLQLHNFPMDEH	163
<i>model-1b</i>	93	IKVLRNLNSNMVGKIWIPTDFFRNSKKADAHWITTPNRMLRIWNDGRVLYTLRLTIDAECQLQLHNFPMDEH	163
<i>model-2a</i>	80	MTVLRNLNLMASKIWTPTDFFHNGKKSVAHNMTMPNKLRLRITDGTLLYTMRLTVRAECPMHLEDFPMDAH	150
<i>model-2c</i>	93	IKVLRNLNSNMVGKIWIPTDFFRNSKKADAHWITTPNRMLRIWNDGRVLYTLRLTIDAECQLQLHNFPMDEH	163
<i>refined-γ_2</i>	93	IKVLRNLNSNMVGKIWIPTDFFRNSKKADAHWITTPNRMLRIWNDGRVLYTLRLTIDAECQLQLHNFPMDEH	163
<i>model-1a</i>	164	SCPLFSSYGYPREEIVYQWKRSSVE-VGDTRSW-RLYQFSFVGLRNTTEVVKTTSGDYVVMVSYFDLSRR	232
<i>model-1b</i>	164	SCPLFSSYGYPREEIVYQWKRSSVE-VGDTRSW-RLYQFSFVGLRNTTEVVKTTSGDYVVMVSYFDLSRR	232
<i>model-2a</i>	151	ACPLKFGSYAYTRAEEVVEWTRPARSVVVAEDGSRLNQYDLLGQTVDSGIVQSSTGEYVVMTHHFLKRR	221
<i>model-2c</i>	164	SCPLFSSYGYPREEIVYQWKRSSVE-VGDTRSW-RLYQFSFVGLRNTTEVVKTTSGDYVVMVSYFDLSRR	232
<i>refined-γ_2</i>	164	SCPLFSSYGYPREEIVYQWKRSSVE-VGDTRSW-RLYQFSFVGLRNTTEVVKTTSGDYVVMVSYFDLSRR	232

Fig. S.I.-2. Comparison of the ClustalX alignments before and after manual alterations of the GABA_AR sequences relative to the structural template alignment. Image is generated with JalView.³³ Columns are colored by conservation at 17% threshold. A) Original (left) and altered (right) alignment in the N-terminal α -helix region. B) Original (left) and altered (right) alignment in the L5-L5' region. C) Original (top) and altered (bottom) alignment in loops F and C.

A)

Ac-AChBP	1	HSQANLMRLKSDLF--NRS--PMYPGP-TK--DDPL	29	1	HSQANLMRLKSDLF--NRS--PMYPGP-TK--DDPL	29
Ls-AChBP	1	----DRADILYNIR-QTS--RPDVIP-TQR-DRPV	26	1	----DRADILYNIR-QTS--RPDVIP-TQR-DRPV	26
Bt-AChBP	1	-----QIRWTL--NQITGESDVIP-LSN-NTPL	25	1	-----QIRWTL--NQITGESDVIP-LSN-NTPL	25
ELIC	1	-----PV	2	1	-----PV	2
GLIC	1	-----VSPPPPIA-DEPL	12	1	-----VSPPPPIA-DEPL	12
M. ACh α 1	1	--SEHETRL EAKLF--EDY--SSVVRP-VEHREIV	29	1	--SEHETRL EAKLF--EDY--SSVVRP-VEHREIV	29
T. ACh α	1	--SEHETRLVANLL--ENY--NKVIRP-VEHHTHFV	29	1	--SEHETRLVANLL--ENY--NKVIRP-VEHHTHFV	29
T. ACh β	1	--SVMEDTLLSVLF--ENY--NPKVRP-SQTVGDKV	29	1	--SVMEDTLLSVLF--ENY--NPKVRP-SQTVGDKV	29
T. ACh γ	1	---NEEGRLEKLL--GDY--DKRIKP-AKTLDHVI	28	1	---NEEGRLEKLL--GDY--DKRIKP-AKTLDHVI	28
T. ACh δ	1	--VNEEERLINDLLIVNKY--NKHVRP-VKHNEEVV	31	1	--VNEEERLINDLLIVNKY--NKHVRP-VKHNEEVV	31
GABA α 1	3	LQDELKDNTTVFTRILDRLLDGYDNRLRPLGLGERVT	38	9	DNTTVFTRILDRLL--DGY--DNRLRP-GLG-ERV	38
GABA β 2	1	--SVNDPSNMSLVKETVDRLLKGYDIRLRFDFGGPPV	35	6	SNMSLVKETVDRLL--KGY--DIRLRF-DFG-GPPV	35
GABA γ 2	16	WVLT PKVPEGDVTVILNLLLEGYDNKLRPDIGVKPT	51	22	VPEGDVTVILNLL--EGY--DNKLRP-DIG-VKPT	51

B)

Ac-AChBP	86	WTPDITAYS-STR--PVQVLSPOI AVVTHDG	113	86	WTPDITAYSSTR--PVQVLSPO---IAVVTHDG	113
Ls-AChBP	81	WV PDLAAYN-AIS--KPEVLTQPQLARVVSDDG	108	81	WV PDLAAYNAIS--KPEVLTQP---LARVVSDDG	108
Bt-AChBP	81	WTPDLSFYNAIA--APELLSADR VVSKDG	108	81	WTPDLSFYNAIA--APELLSAD---RVVSKDG	108
ELIC	62	WVPALEFIN-VVG--SPDT-GNKRLMLFPDG	88	62	WVPALEFINVVG--SPDT-GNK---RLMLFPDG	88
GLIC	68	WIPEIRFVN-VEN--ARDA-DVVDISVSPDG	94	68	WIPEIRFVNVEN--ARDA-DVV--DISVSPDG	94
M. ACh α 1	86	WRPDVVLVN-NADGDFAIV-KFTKVL LDYTG	114	86	WRPDVVLVNNADGDFAIV-KFT---KVL LDYTG	114
T. ACh α	86	WLPDLVLYN-NADGDFAIV-HMTKLL LDYTG	114	86	WLPDLVLYNNADGDFAIV-HMT---KLL LDYTG	114
T. ACh β	86	WQPDIVLVMN-NNDGSFEIT-LHVNVLVQHTG	114	86	WQPDIVLVMNNDGSFEIT-LHV---NVLVQHTG	114
T. ACh γ	85	WLPDVVLEN-NVDGQFEVA-YYANVLYNDG	113	85	WLPDVVLENNVDGQFEVA-YYA---NVLVYNDG	113
T. ACh δ	88	WIPDIVLQNNNDGQYNVA-YFCNVLVRPNDG	116	88	WIPDIVLQNNNDGQYNVA-YFC---NVLVRPNDG	116
GABA α 1	94	WTPDTFFHNGKKSVAHNMTMPNKLRLITEDG	124	94	WTPDTFFHNGKK--SVAHNMTMPNKLRLITEDG	124
GABA β 2	91	WV PDTYFLNDKKS FVHGVTVKNRMLRHPDG	121	91	WV PDTYFLNDKK--SFVHGVTVKNRMLRHPDG	121
GABA γ 2	107	WIPDTFFRNSKKADAHWITPNRMLRIWNDG	137	107	WIPDTFFRNSKK--ADAHWITPNRMLRIWNDG	137

C)

Ac-AChBP	154	IDLK-TDTD-Q-V-DLSSYY----ASSKYEILSATQTRQVQHYSCCP-----EPYIDV	198
Ls-AChBP	149	ISVD-PTTE-N-SDDSEYFS----QYSRFEILDVTQKKNVSYSCCP-----EAYEDV	194
Bt-AChBP	149	FALITGEEGV-VNIAEYFD----SPKFDLLSATQSLNRKKYSCE-----NMYDDI	194
ELIC	128	QQLRF--SD--I-QVY-TENIDNEEIDEWIRKASTHISDIRYDHLSSVQPNQNEFSRI	180
GLIC	136	IVLA-VDLE-K-V-GK-NDD----VFLTGWDIESFTAVVKPANFALED-----RLESKL	180
M. ACh α 1	156	VAIN-PESD-Q-P-DLSNFM----ESGEWVKEARGWKHWVYSCCP-----TTPYLDI	201
T. ACh α	156	VSIS-PESD-R-P-DLSTFM----ESGEWVMKDYRGWKHWVYTCPP-----DTPYLDI	201
T. ACh β	156	VILQ-HALDA-M-I-NQDAFT----ENGQWSIEHKPSRKNWRS-----DPSYEDV	198
T. ACh γ	155	VNLQ-LSAE-EGI-DPEDFT----ENGWETIRHRPAKKKNYNWQLTKD-----DIDFQEI	201
T. ACh δ	158	ISMD-L----I-I-DPEAFT----ENGWEI I HKPAKKNIYGDKFPN-----GTNYQDV	200
GABA α 1	166	VVYEWTRPAR--SVVVAEDGS--RLNQYDL LGQTVDSGIVQSSSTGE-----YVVM	212
GABA β 2	163	IEFYWRGDDN----AVTGVT--KIELPQFSIVDYKLITKKYVVFSTGS-----YPRL	207
GABA γ 2	179	IVYQWKRSS----VEVGDTRS--WRLYQFSFVGLRNTTEVVKTTSGD-----YVVM	223

Ac-AChBP	154	IDLK-TDTD-Q-V--DLSSYY----ASSKYEILSATQTRQVQHYSCCP-----EPYIDV	198
Ls-AChBP	149	ISVD-PTTE-N-S-DDSEYFS----QYSRFEILDVTQKKNVSYSCCP-----EAYEDV	194
Bt-AChBP	149	FALITGEEGV-VNIAEYFD----SPKFDLLSATQSLNRKKYSCE-----NMYDDI	194
ELIC	128	QQLRF--SD--I-QVY-TENIDNEEIDEWIRKASTHISDIRYDHLSSVQPNQNEFSRI	180
GLIC	136	IVLA-VDLE-K-V--GK-NDD----VFLTGWDIESFTAVVKPANFALED-----RLESKL	180
M. ACh α 1	156	VAIN-PESD-Q-P-DLSNFM----ESGEWVKEARGWKHWVYSCCP-----TTPYLDI	201
T. ACh α	156	VSIS-PESD-R-P-DLSTFM----ESGEWVMKDYRGWKHWVYTCPP-----DTPYLDI	201
T. ACh β	156	VILQ-HALDAM-I--NQDAFT----ENGQWSIEHKPSRKNWRS-----DPSYEDV	198
T. ACh γ	155	VNLQ-LSAE-EGI--DPEDFT----ENGWETIRHRPAKKKNYNWQLTKD-----DIDFQEI	201
T. ACh δ	158	ISMD-L----I-I--DPEAFT----ENGWEI I HKPAKKNIYGDKFPN-----GTNYQDV	200
GABA α 1	166	VVYE-WTRE-P-ARSVVVAEDGS--RLNQYDL LGQTVDSGIVQSS--T-----GEYVVM	212
GABA β 2	163	IEFY-WRGD-D-NAVTVTKI----ELPQFSIVDYKLITKKVVFSS--T-----GSYPRL	207
GABA γ 2	179	IVYQ-WKRS-S-VE-VGDTRSW--RLYQFSFVGLRNTTEVVKTT--S-----GDYVVM	223

Fig. S.I.-3: Ramachandran plot for the refined model. Triangles represent Gly residues. Generated with Procheck.³⁴

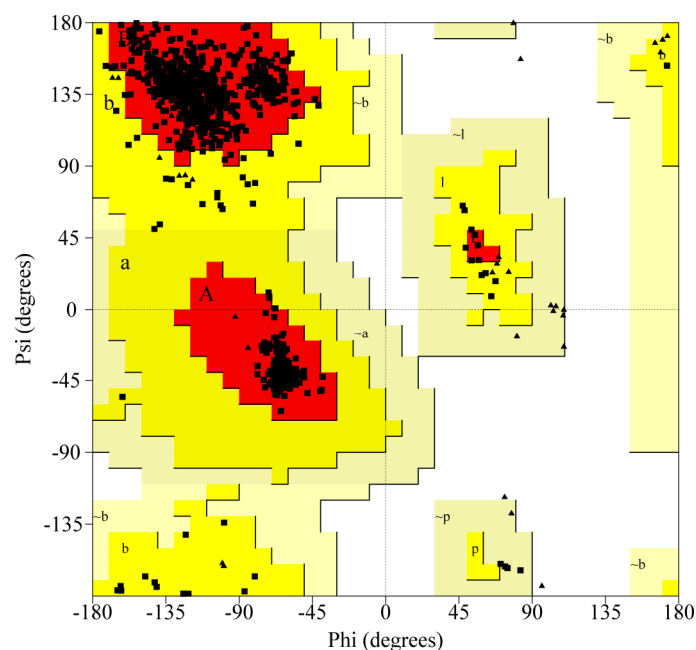


Fig. S.I.-4: ProSA-web³⁵ analysis of the local model quality, showing the improvements from the initial (black) to the refined model (red). This can also be thought of as the individual residue contributions to the z-score. In general, regions above zero in the shown plots indicate potentially problematic regions. β_2 subunit comparison (chain A) to the initial model 1a is shown to the left, and α_1 subunit comparison (chain B) to initial model 1b is shown to the right. A z-score (“knowledge-based energy”) is calculated for each residue, however to improve readability the plot is smoothed using two different window sizes (10 and 40). With window size 40, the average score is calculated for each 40-residue interval ($i, i+39$) and assigned to the central residue ($i+19$) of that interval.

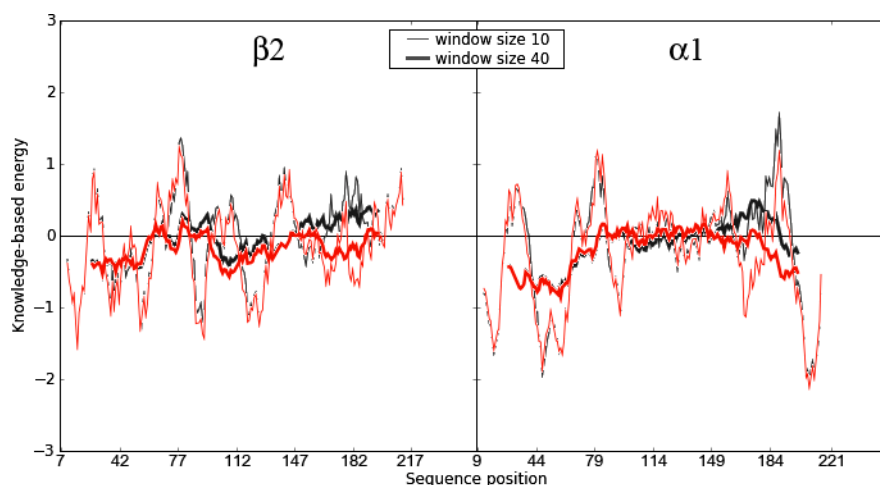
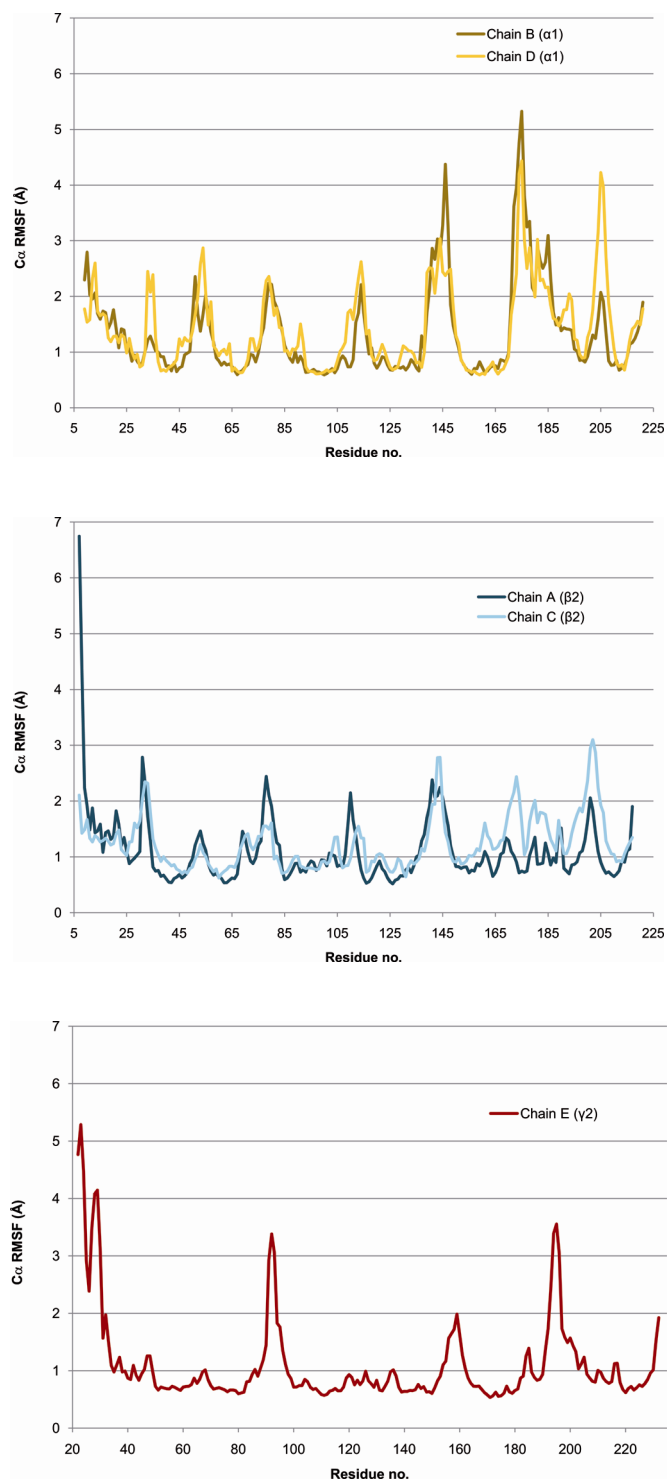


Fig. S.I.-5. Chain and residue specific C α RMSF for the production MD simulation.

Reference List

1. Sali A, Blundell TL. Comparative protein modelling by satisfaction of spatial restraints. *J Mol Biol* 1993;234:779-815.
2. Maestro. New York, NY: Schrödinger, LLC; 2009.
3. Boileau AJ, Evers AR, Davis AF, Czajkowski C. Mapping the agonist binding site of the GABA_A receptor: Evidence for a β -strand. *J Neurosci* 1999;19:4847-4854.
4. Holden JH, Czajkowski C. Different residues in the GABA_A receptor α_1 T60- α_1 K70 region mediate GABA and SR-95531 actions. *J Biol Chem* 2002;277:18785-18792.
5. Jansen M, Rabe H, Strehless A, Dieler S, Debus F, Dannhardt G, Akabas MH, Luddens H. Synthesis of GABA_A receptor agonists and evaluation of their α -subunit selectivity and orientation in the GABA binding site. *J Med Chem* 2008;51:4430-4448.
6. Schrödinger Suite 2009 Protein Preparation Wizard; Epik version 2.0, Schrödinger, LLC, New York, NY, 2009; Impact version 5.5, Schrödinger, LLC, New York, NY, 2009; Prime version 2.1, Schrödinger, LLC, New York, NY, 2009.
7. Jorgensen WL, Chandrasekhar J, Madura JD, Impey RW, Klein ML. Comparison of simple potential functions for simulating liquid water. *J Chem Phys* 1983;79:926-935.
8. Goodford PJ. A computational procedure for determining energetically favorable binding sites on biologically important macromolecules. *J Med Chem* 1985;28:849-857.
9. GRID. Pinner, Middlesex: Molecular Discovery, Ltd.; 2005.
10. Berendsen HJC, Postma JPM, van Gunsteren WF, DiNola A, Haak JR. Molecular dynamics with coupling to an external bath. *J Chem Phys* 1984;81:3684-3690.
11. Nosé S. A molecular dynamics method for simulations in the canonical ensemble. *Mol Phys* 1984;52:255-268.
12. Martyna GJ, Tobias DJ, Klein ML. Constant pressure molecular dynamics algorithms. *J Chem Phys* 1994;101:4177-4189.
13. Ryckaert JP, Ciccotti G, Berendsen HJC. Numerical integration of the cartesian equations of motion of a system with constraints: molecular dynamics of n-alkanes. *J Comput Phys* 1977;23:327-341.
14. Essmann U, Perera L, Berkowitz ML, Darden T, Lee H, Pedersen LG. A smooth particle mesh Ewald method. *J Chem Phys* 1995;103:8577-8593.
15. Kryshchukovych A, Venclovas C, Fidelis K, Moulton J. Progress over the first decade of CASP experiments. *Proteins* 2005;61 Suppl 7:225-236.
16. Campagna-Slater V, Weaver DF. Molecular modelling of the GABA_A ion channel protein. *J Mol Graph Model* 2007;25:721-730.

17. Harrison NJ, Lummis SC. Molecular modeling of the GABA_C receptor ligand-binding domain. *J Mol Model* 2006;12:317-324.
18. Ernst M, Brauchart D, Boresch S, Sieghart W. Comparative modeling of GABA_A receptors: Limits, insights, future developments. *Neuroscience* 2003;119:933-943.
19. Ernst M, Bruckner S, Boresch S, Sieghart W. Comparative models of GABA_A receptor extracellular and transmembrane domains: Important insights in pharmacology and function. *Mol Pharmacol* 2005;68:1291-1300.
20. Adamian L, Gussin HA, Tseng YY, Muni NJ, Feng F, Qian H, Pepperberg DR, Liang J. Structural model of $\rho 1$ GABA_C receptor based on evolutionary analysis: Testing of predicted protein-protein interactions involved in receptor assembly and function. *Protein Sci* 2009;18:2371-2383.
21. Melis C, Lummis SC, Molteni C. Molecular dynamics simulations of GABA binding to the GABA_C receptor: The role of Arg104. *Biophys J* 2008;95:4115-4123.
22. Mokrab Y, Bavro VN, Mizuguchi K, Todorov NP, Martin IL, Dunn SM, Chan SL, Chau PL. Exploring ligand recognition and ion flow in comparative models of the human GABA type A receptor. *J Mol Graph Model* 2007;26:760-774.
23. Law RJ, Lightstone FC. Modeling neuronal nicotinic and GABA receptors: Important interface salt-links and protein dynamics. *Biophys J* 2009;97:1586-1594.
24. Hall TA. BioEdit: a user-friendly biological sequence alignment editor and analysis program for Windows 95/98/NT. *Nucleic Acids Symp Ser* 1999;41:95-98.
25. Newell JG, Czajkowski C. The GABA_A Receptor α_1 Subunit Pro174-Asp191 Segment Is Involved in GABA Binding and Channel Gating. *J Biol Chem* 2003;278:13166-13172.
26. Amin J, Weiss DS. GABA_A receptor needs two homologous domains of the β -subunit for activation by GABA but not by pentobarbital. *Nature* 1993;366:565-569.
27. Wagner DA, Czajkowski C. Structure and dynamics of the GABA binding pocket: A narrowing cleft that constricts during activation. *J Neurosci* 2001;21:67-74.
28. Friesner RA, Banks JL, Murphy RB, Halgren TA, Klicic JJ, Mainz DT, Repasky MP, Knoll EH, Shelley M, Perry JK, Shaw DE, Francis P, Shenkin PS. Glide: a new approach for rapid, accurate docking and scoring. 1. Method and assessment of docking accuracy. *J Med Chem* 2004;47:1739-1749.
29. Frølund B, Jørgensen AT, Tagmose L, Stensbøl TB, Vestergaard HT, Engblom C, Kristiansen U, Sanchez C, Krogsgaard-Larsen P, Liljefors T. Novel class of potent 4-arylalkyl substituted 3-isoxazolol GABA_A antagonists: Synthesis, pharmacology, and molecular modeling. *J Med Chem* 2002;45:2454-2468.
30. Frølund B, Jensen LS, Guandalini L, Canillo C, Vestergaard HT, Kristiansen U, Nielsen B, Stensbøl TB, Madsen C, Krogsgaard-Larsen P, Liljefors T. Potent 4-aryl- or 4-arylalkyl-substituted 3-isoxazolol GABA_A antagonists: Synthesis, pharmacology, and molecular modeling. *J Med Chem* 2005;48:427-439.

31. Frølund B, Jensen LS, Storustovu SI, Stensbøl TB, Ebert B, Kehler J, Krosgaard-Larsen P, Liljefors T. 4-aryl-5-(4-piperidyl)-3-isoxazolol GABA_A antagonists: Synthesis, pharmacology, and structure-activity relationships. *J Med Chem* 2007;50:1988-1992.
32. Møller HA, Sander T, Kristensen JL, Nielsen B, Krall J, Bergmann ML, Christiansen B, Balle T, Jensen AA, Frølund B. Novel 4-(piperidin-4-yl)-1-hydroxypyrazoles as γ -aminobutyric acid_A receptor ligands: Synthesis, pharmacology, and structure-activity relationships. *J Med Chem* 2010;53:3417-3421.
33. Clamp M, Cuff J, Searle SM, Barton GJ. The Jalview Java alignment editor. *Bioinformatics* 2004;20:426-427.
34. Laskowski RA, MacArthur MW, Moss DS, Thornton JM. PROCHECK: a program to check the stereochemical quality of protein structures. *J Appl Cryst* 1993;26:283-291.
35. Wiederstein M, Sippl MJ. ProSA-web: interactive web service for the recognition of errors in three-dimensional structures of proteins. *Nucleic Acids Res* 2007;35:W407-W410.